Int. J. Heat Mass Transfer. Vol. 35, No. 7, pp. 1771–1778, 1992
Printed in Great Britain

0017–9310/92 $5.00 + 0.00

Interaction between shrinkage-induced fluid flow and natural convection during alloy solidification

K. C. CHIANG and H. L. TSAI

Department of Mechanical and Aerospace Engineering and Engineering Mechanics, University of Missouri–Rolla, Rolla, MO 65401, U.S.A.

(*Received* 19 *October* 1990 *and in final form* 7 *June* 1991)

Abstract—Solidification of alloys in a two-dimensional rectangular cavity with riser is analyzed. Results for the following three cases are presented: (1) natural convection due to a temperature gradient with constant domain; (2) shrinkage-induced fluid flow with domain change; and (3) interactions between cases (1) and (2). For the alloy under study (1% Cr–steel), it is found that at the beginning and the final stage of solidification, the shrinkage-induced fluid flow is stronger than the natural convection, while in the middle stage of solidification the natural convection dominates. Also, the fluid flow caused by shrinkage in the mushy zone is more significant than that by natural convection, which implies that the shrinkage effect should be included in the modeling if the prediction of flow-related casting defects is desired.

INTRODUCTION

FLUID flow in a solidifying casting can be caused by the density difference between the solid and the liquid phases (shrinkage-induced flow), the thermal and/or solutal gradients in the presence of gravity (natural convection), external forces (centrifugal force, magnetic force, etc.), and the surface tension gradient at the free surface (Marangoni effect). It has long been recognized that fluid flow plays an important role in the formation of casting defects (e.g. refs. [1, 2]). In particular, it has been reported that the interdendritic fluid flow in the mushy zone is the general cause for the formation of macrosegregation and porosity in castings. Hence, a detailed knowledge of fluid flow patterns and heat transfer characteristics during solidification is crucial to the proper control of casting quality.

In the past, a great deal of effort has been devoted to establishing mathematical models for the prediction of fluid flow and the associated defect formation in castings. However, the modeling of fluid flow and heat transfer for a phase change system is inherently difficult, due to the presence of the solid phase, mushy zone, and liquid phase, as well as the release of latent heat at the unknown solid–liquid interfaces. In spite of the difficulties, tremendous progress has been made in the past in the modeling of casting solidification. A comprehensive review of mathematical–numerical models in the solid–liquid phase change can be found in the literature (e.g. ref. [3]).

The historical development of casting solidification models can be generally divided into three periods. In the first period, roughly before 1970, the studies were concentrated on heat conduction with phase change problems (e.g. ref. [4]). In order to study casting defects, the fluid flow was usually prescribed (or from experiments) and decoupled from the energy equation. As a result, the models were limited to the one-dimensional case (e.g. ref. [5]). In the second period, up to the middle of the 1980s, the coupling of the momentum equation with the energy equation was attempted (e.g. refs. [6–8]). The influence of interdendritic fluid flow on the formation of macrosegregation was investigated. However, usually the simple Darcy's law was employed, instead of solving the complete momentum equation, to obtain the velocity field. In addition, the coupling between the solid, mushy, and liquid regions was either ignored or treated by means of the multiple-region method. In such an approach, separate conservation equations are derived and solved for each region, and an appropriate energy balance at the interfaces is then employed to couple the solutions. The modeling requires a prescription of the size and shape of the mushy region, and the associated interfaces with the solid and liquid regions (e.g. ref. [8]). Hence, the multiple-region method is limited to some cases with the assumption of quasi-steady state or simple geometry.

In the third period, late 1980s to the present, the continuum (single region) concept, based on the classical mixture theory or the volume averaging technique, was proposed (e.g. refs. [9–11]). The continuum approach employs a single set of conservation equations, which are applicable to the entire domain including the solid phase, mushy zone, and liquid phase. Thus, it avoids tracking the phase interface and the explicit consideration of the interfacial boundary conditions. The continuum concept has been used to model the formation of macrosegregation with moderate success when compared with the experimental results [9, 10].

NOMENCLATURE

C	coefficient, equation (1)
g	gravitational acceleration
H	height of casting, Fig. 1
H_1	height of riser and casting, Fig. 1
K	permeability
L	length of casting, Fig. 1
L_1	length of riser, Fig. 1
p	pressure
t	time
T	temperature
T_l	liquidus temperature
v	velocity component in the y direction
$\mathbf{V}$	velocity vector
x	horizontal coordinate
y	vertical coordinate.

Greek symbols

β	thermal expansion coefficient
μ	dynamic viscosity
ρ	density.

Subscripts

b	bottom wall of cavity
i	initial condition
l	liquid phase
r	relative velocity or right-side wall of cavity
s	solid phase.

None of the above-mentioned solidification models had rigorously considered the shrinkage effect until recently, when the authors [12] established a mathematical model to calculate the fluid flow and domain change caused by shrinkage. However, in that study the natural convection induced by a temperature gradient was neglected. In the present study, the fluid flow and heat transfer will be investigated for the following three cases: (1) natural convection due to temperature gradient with constant domain; (2) shrinkage-induced fluid flow with domain change; and (3) interactions between cases (1) and (2).

ANALYSIS

Consider the solidification of an alloy, placed in a rectangular cavity, extending from $x = 0$ to $x = L$ and from $y = 0$ to $y = H$, as shown in Fig. 1. A riser is located at the top of the casting, extending from $x = 0$ to $x = L_1$ and from $y = H$ to $y = H_1$. Initially the casting and the riser are occupied by molten alloy at a uniform temperature T_i, which is higher than the liquidus temperature T_l. Then, at time $t = 0$ the planes corresponding to $y = 0$ and $x = L$ are suddenly brought to temperatures T_b and T_r, respectively, with $T_b < T_r$, which are below the solidus temperature T_s, while all the other surfaces are insulated.

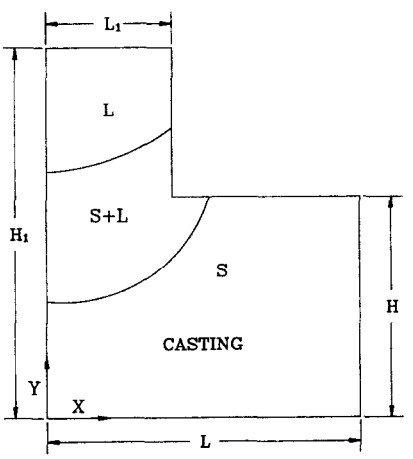

FIG. 1. Schematic of the physical domain and the coordinate system.

The continuum equations developed by Bennon and Incropera [9] have been modified to include the shrinkage-induced fluid flow. The detailed derivation and the associated assumptions of the governing system of equations can be found in refs. [12, 13]. The continuity equation, x-momentum equation, energy equation, and the associated auxiliary equations are exactly the same as those given in ref. [12], and they will not be repeated here. However, as the natural convection due to a temperature gradient is included

Table 1. Thermophysical properties for 1% Cr–steel, casting conditions, and geometric data

Symbol (units)	Value
k_s (cal cm^{-1} s^{-1} K^{-1})	0.07852
k_l (cal cm^{-1} s^{-1} K^{-1})	0.06861
c_s (cal g^{-1} K^{-1})	0.15560
c_l (cal g^{-1} K^{-1})	0.15550
ρ_s (g cm^{-3})	7.36260
ρ_l (g cm^{-3})	6.96830
$\rho_s = \rho_l$ (g cm^{-3})	7.16545†
Δh (cal g^{-1})	65.9033
T_s (K)	1744.4
T_l (K)	1777.7
T_i (K)	1843.15
T_b (K)	1200
T_r (K)	1700
μ (g cm^{-1} s^{-1})	4.4122×10^{-3}
β (K^{-1})	7.85579×10^{-9}‡
L (cm)	10.0
L_1 (cm)	2.0
H (cm)	8.0
H_1 (cm)	20.0

† Density for case (1), natural convection with constant domain.
‡ Assumed.

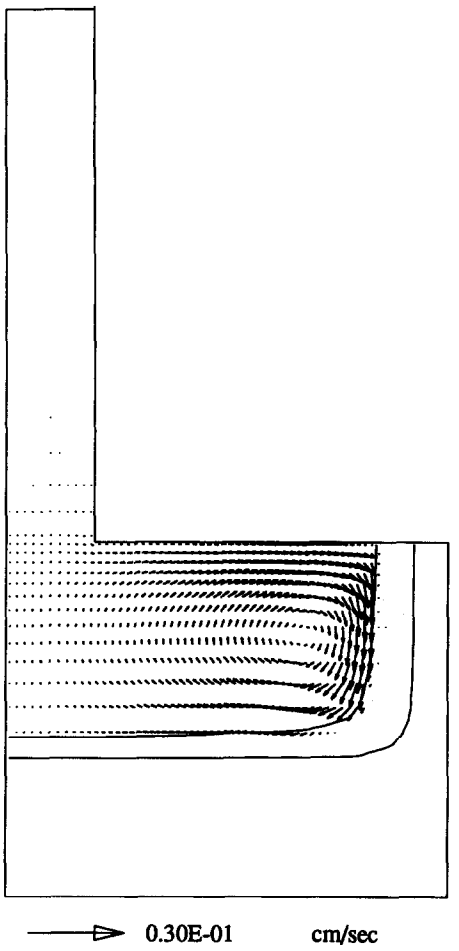

FIG. 2(a). The predicted flow patterns and mushy zone for case (1) at time $t = 96.5$ s.

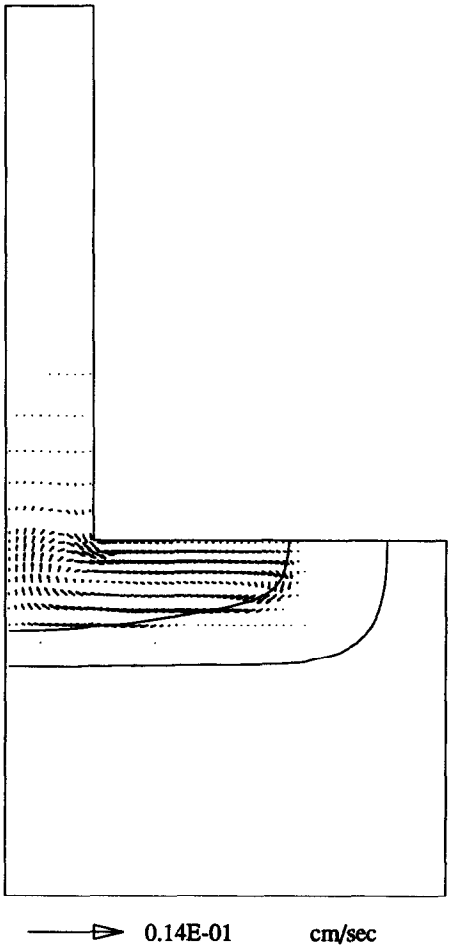

FIG. 2(b). The predicted flow patterns and mushy zone for case (1) at time $t = 265.5$ s.

in the present study, the y-momentum equation is modified to

$$\frac{\partial}{\partial t}(\rho v)+\nabla\cdot(\rho\mathbf{V}v)=\nabla\cdot\left(\mu_l\frac{\rho}{\rho_l}\nabla v\right)-\frac{\partial p}{\partial y}$$
$$-\frac{\mu_l}{K}\frac{\rho}{\rho_l}(v-v_s)-\frac{C\rho^2}{K^{1/2}\rho_l}|v-v_s|(v-v_s)$$
$$-\nabla\cdot(\rho f_s f_l\mathbf{V}_r v_r)+\nabla\cdot\left(\mu_l v\nabla\left(\frac{\rho}{\rho_l}\right)\right)+\rho g\beta(T-T_l) \quad (1)$$

where the last term on the right-hand side of equation (1) is new and is caused by natural convection using the Boussinesq approximation. As discussed in ref. [12], the shrinkage-induced fluid flow is accounted for by the second last term on the right-hand side of equation (1). Hence, one can study the effects of shrinkage and/or natural convection by maintaining or omitting the corresponding terms in equation (1).

As explained before, for the casting geometry illustrated in Fig. 1, the boundary conditions can be summarized as

(1) at $x = 0$ and $0 \leqslant y \leqslant H_1$:

$$u = 0, \quad v = 0, \quad \partial T/\partial x = 0 \quad (2a)$$

(2) at $x = L$ and $0 \leqslant y \leqslant H$:

$$u = 0, \quad v = 0, \quad T = T_r \quad (2b)$$

(3) at $x = L_1$ and $H \leqslant y \leqslant H_1$:

$$u = 0, \quad v = 0, \quad \partial T/\partial x = 0 \quad (2c)$$

(4) at $y = 0$ and $0 \leqslant x \leqslant L$:

$$u = 0, \quad v = 0, \quad T = T_b \quad (3a)$$

(5) at $y = H$ and $L_1 \leqslant x \leqslant L$:

$$u = 0, \quad v = 0, \quad \partial T/\partial y = 0 \quad (3b)$$

(6) at $y = H_1$ and $0 \leqslant x \leqslant L_1$:

$$p = 0, \quad \partial u/\partial y = 0, \quad \partial T/\partial y = 0 \quad (3c)$$

where pressure p is the gage pressure. In the calculation of fluid flow due to natural convection, the boundary conditions are the same as equations (2) and (3) except that equation (3c) is replaced by

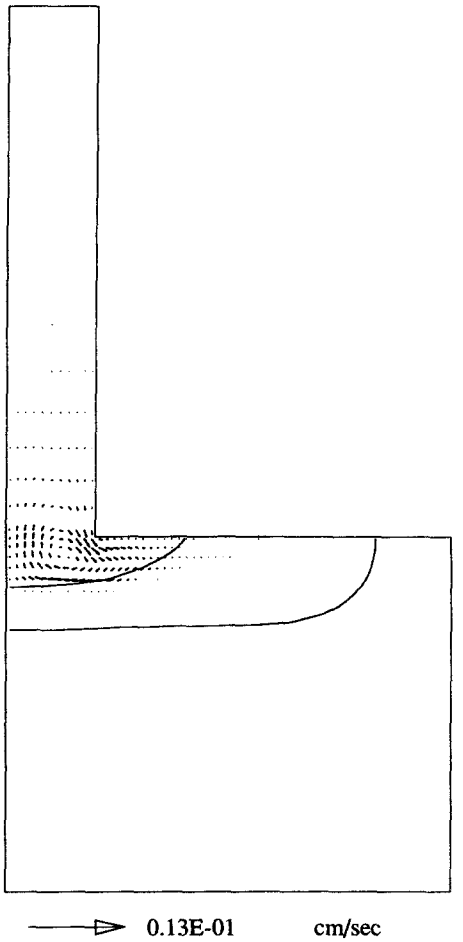

FIG. 2(c). The predicted flow patterns and mushy zone for case (1) at time $t = 336.5$ s.

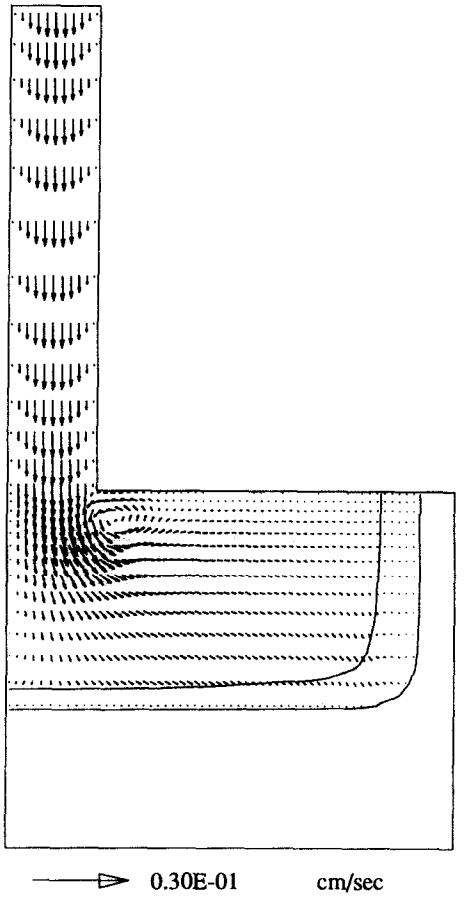

FIG. 3(a). The predicted flow patterns and mushy zone for case (2) at time $t = 96.5$ s.

(7) at $y = H_1$ and $0 \leqslant x \leqslant L_1$:

$$u = 0, \quad v = 0, \quad \partial T/\partial y = 0. \tag{3d}$$

The system of governing equations was solved by the SIMPLEC algorithm. The details of the solution procedure and the check of solution accuracy have been discussed in ref. [11], and they will not be repeated here.

RESULTS AND DISCUSSION

Numerical calculations were performed with typical material properties for 1% Cr–steel [14]. These properties, casting conditions, and geometric data are summarized in Table 1. Calculations were performed for the following cases: (1) natural convection due to temperature gradient with constant domain; (2) shrinkage-induced fluid flow with domain change; and (3) interactions between cases (1) and (2). The velocity vectors to be shown next are based on the continuum velocity components u and v. Since the velocity of the solid phase, $\mathbf{V}_s$, is assumed to be zero, u and v can be alternately expressed as $f_l u_l$ and $f_l v_l$, respectively. Hence, velocities appearing in the pure liquid region are actual velocities, while those appearing in the mushy region are the superficial or seepage velocities. Solidus and liquidus contours are also shown on the velocity plots, and they represent, respectively, the boundaries of the solid and mushy regions, and the mushy and liquid regions.

Case (1). *Natural convection due to a temperature gradient with constant domain*

In this case, the average of solid phase density and liquid phase density at the liquidus temperature is adopted in the calculations. As there is no density difference between the solid and liquid phases, and the thermal expansion coefficient is small for this case, the calculation domain remains constant, which is the same as the traditional assumption on phase change problems [9–11].

The transient development of the solidus and liquidus contours, and the fluid flow are shown in Figs. 2(a) (c) at times $t = 96.5$, 256.5, and 336.5 s, respectively. The fluid in the casting adjacent to the cold, right-side wall is driven vertically downward due to

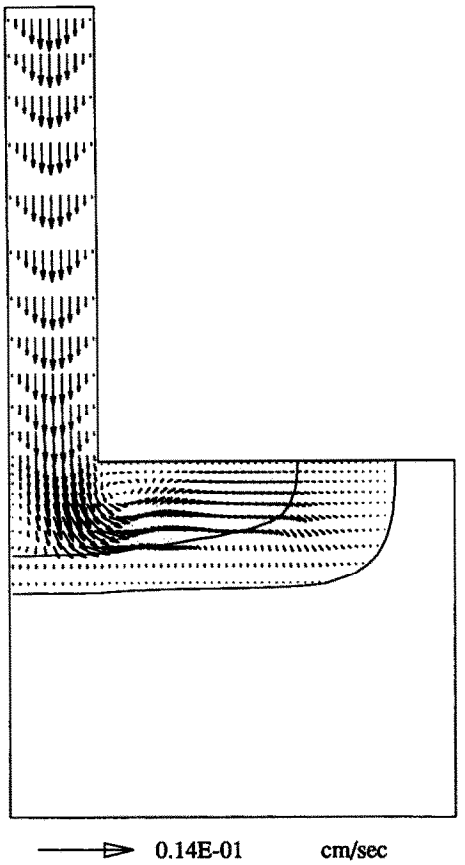

FIG. 3(b). The predicted flow patterns and mushy zone for case (2) at time $t = 256.5$ s.

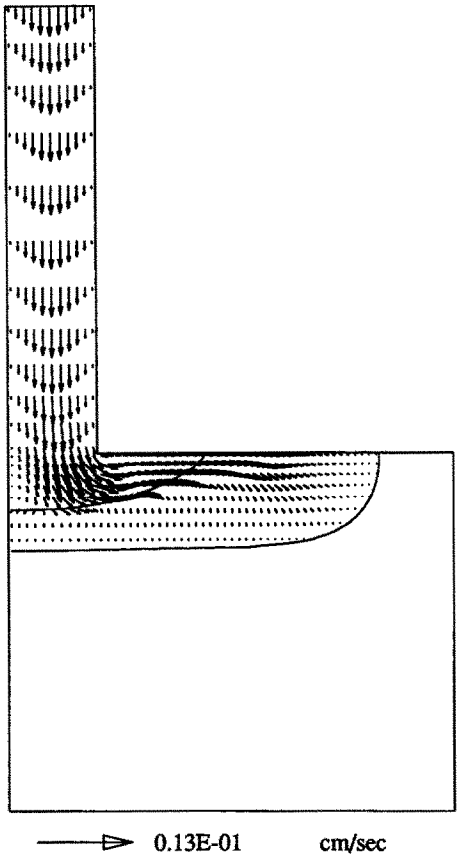

FIG. 3(c). The predicted flow patterns and mushy zone for case (2) at time $t = 336.5$ s.

the presence of a temperature gradient. This descending fluid collides with the solid front near the bottom wall and is deflected. A weak clockwise recirculating vortex is then formed, as shown in Fig. 2(a). The fluid within the riser is almost stagnant, because the recirculating cell within the casting is weak and the increasing temperature toward the top of the riser decreases the natural convection effect within the riser. The solidus contour near the bottom wall is propagated faster than that near the right-side wall, because the imposed temperature at the bottom wall T_b is lower than that of the right-side wall T_r. From Figs. 2(a)–(c), one also sees that the fluid flow within the mushy region is much smaller than that in the liquid phase, and the size of the mushy zone increases with time.

Due to the moving of the solid front from the bottom wall, the flow field gradually extends to the bottom of the riser, and the recirculating vortex is compressed into an elliptic shape by the solid front from the bottom wall, as shown in Fig. 2(b). At the final stage of solidification (Fig. 2(c)), the solidus and liquidus fronts are almost parallel to the x-axis, and the fluid flow due to natural convection is nearly diminished.

Case (2). *Shrinkage-induced fluid flow with domain change*

Figures 3(a)–(c) illustrate the velocity, the solid front, and the liquid front for case (2) at times $t = 96.5$, 256.5, and 336.5 s, respectively. At the beginning of solidification, as the heat flux from the bottom and the right-side walls is very large, the solid fronts are propagated rapidly. Hence, the shrinkage-induced fluid flow is relatively large at the early stage of solidification. The liquid metal in the riser is driven downward to feed such shrinkage, as illustrated in Fig. 3(a), and a counter-clockwise recirculating vortex is formed just at the intersection of the riser and the casting. The creation of the vortex is due to a sudden expansion of the area at this location. At a later time, as shown in Fig. 3(b), the shrinkage-induced fluid flow becomes weaker due to the formation of the solid phase, which increases the thermal resistance and decreases the heat extracting rate. The strength of shrinkage-induced fluid flow is further decreased as time increases, and finally, the recirculating cell is diminished (Fig. 3(c)) as the formation of the solid phase progresses.

One should note that the maximum velocity of the fluid flow always occurs at the top of the riser for the

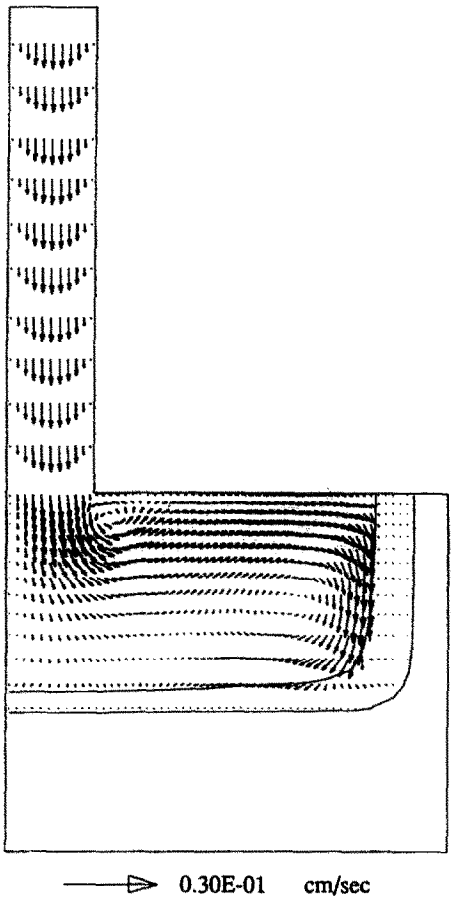

FIG. 4(a). The predicted flow patterns and mushy zone for case (3) at time $t = 96.5$ s.

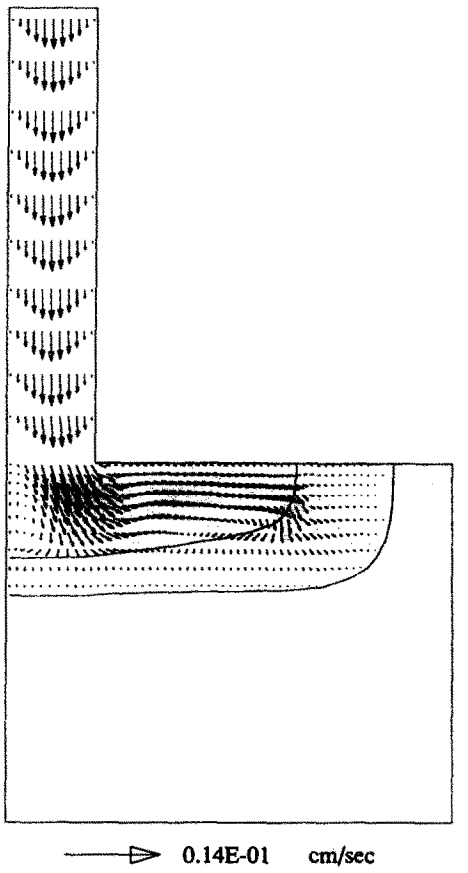

FIG. 4(b). The predicted flow patterns and mushy zone for case (3) at time $t = 256.5$ s.

case of flow induced by shrinkage. In contrast, for the natural convection, case (1), the maximum velocity is usually located near the interface between the pure liquid and the mushy region. The fluid flow within the riser is almost stagnant in case (1), but the flow with greater velocity is found within the riser in case (2). Also, by comparing Figs. 2(b) and (c) and Figs. 3(b) and (c), one finds that the shrinkage-induced fluid flow within the mushy region is larger than that of the case for natural convection. This implies that in the investigation of casting defects, the shrinkage-induced fluid flow cannot be neglected for the conditions used in the present study.

Case (3). *Interactions between case* (1) *and case* (2)

The temporal evolution of fluid flow due to the interactions between case (1) and case (2) is shown in Figs. 4(a)–(c). From Fig. 4(a), time $t = 96.5$ s, one can see that there is a recirculating cell near the intersection of the casting and the riser, which is due to shrinkage-induced fluid flow. Another stronger recirculating cell due to natural convection within the casting can also be seen in Fig. 4(a). The recirculating cell due to shrinkage has disappeared in Fig. 4(b), as this counter-clockwise recirculating cell is balanced by the clockwise recirculating cell due to natural convection. The recirculating cell due to natural convection is nearly diminished at time $t = 256.5$ s (Fig. 4(b)), and a small recirculating cell caused by the interactions between shrinkage-induced fluid flow and natural convection is formed near the bottom of the riser and adjacent to the left-side wall. At the final stage of solidification (Fig. 4(c)), all the recirculating cells have disappeared, and the flow pattern becomes similar to the one found in Fig. 3(c), which is due to shrinkage only.

By comparing the figures (and some other figures which are not shown in this paper [13]) for the three cases discussed above, one can find that the shrinkage-induced fluid flow is dominant at the early stage of solidification because of a large heat flux (or heat extracting rate). At the next stage of solidification, the strength of natural convection is increased and the natural convection tends to become fully developed. Also, the formation of the solid phase increases the thermal resistance, which in turn decreases the heat extracting rate and the shrinkage-induced fluid flow. Thus, the natural convection becomes dominant. At the final stage of solidification, the temperature is almost stratified and increases toward the riser, so

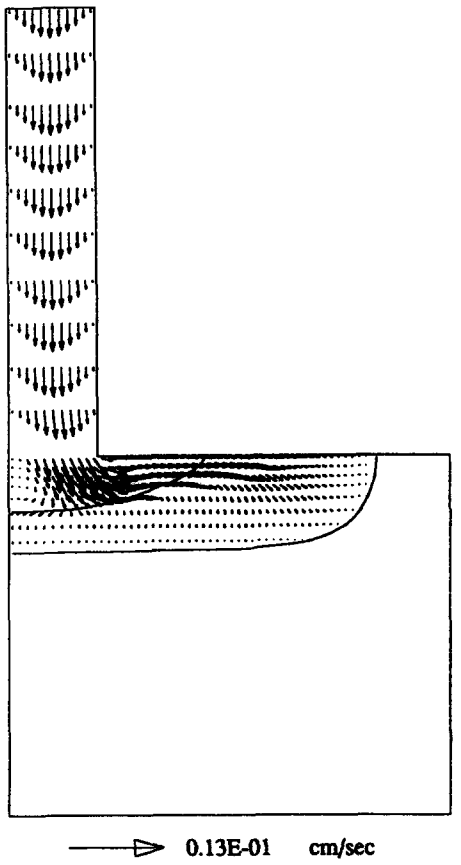

FIG. 4(c). The predicted flow patterns and mushy zone for case (3) at time $t = 336.5$ s.

that natural convection becomes insignificant. At this time, shrinkage-induced fluid flow, although its strength is very weak, once more dominates the flow field.

For the three cases under study, despite the large difference in the flow field, it was found that their isotherms are almost the same [13]. This is mainly due to the high thermal conductivity typically found in many alloys, as well as the small thermal expansion coefficient and density difference between the solid and the liquid phases. This finding is significant because, although the solidification pattern and casting shake-out time depend mainly on the temperature field, several casting defects are closely related to the fluid flow only. Many alloys shrink by 3–7% in volume during solidification. The inclusion of the shrinkage effect in the modeling, perhaps, does not influence the prediction of solidification patterns in castings, but it could significantly affect the prediction of casting defects.

CONCLUSIONS

A mathematical model with which to study the interactions between shrinkage-induced fluid flow and natural convection has been developed. From the numerical calculations for the 1% Cr–steel, several conclusions can be drawn as follows.

1. Although the isotherms and the temperature field in the casting caused by shrinkage and/or natural convection are nearly the same, their flow patterns are very different.
2. The shrinkage-induced fluid flow is significant at the beginning of solidification due to the existence of a large heat flux. In the next stage of solidification, natural convection becomes important because the thermal resistance increases due to the formation of the solid phase, the heat extracting rate decreases as a result, and the natural convection becomes fully developed. At the final stage of solidification, the temperature is almost stratified and increases toward the riser. Therefore, the natural convection effect is almost diminished, and the shrinkage-induced fluid flow, although its strength is very weak, again becomes significant.
3. The fluid flow in the mushy region caused by shrinkage is more significant than that by natural convection due to a temperature gradient. Thus, to study the formation of casting defects, such as porosity and macrosegregation, the shrinkage effect may have to be considered.

Acknowledgements—This study was supported in part by the National Science Foundation under Grant No. CBT-8808212, which is gratefully acknowledged. The authors would like to thank Dr T. S. Chen for his valuable suggestions during the early stage of the present work and in the preparation of the manuscript.

REFERENCES

1. M. C. Flemings, *Solidification Processing*. McGraw-Hill, New York (1974).
2. K. M. Fisher. The effects of fluid flow on the solidification of industrial castings and ingots, *PCH PhysicoChemical Hydrodynamics* **2,** 311–326 (1981).
3. R. Viskanta, Heat transfer during melting and solidification of metals, *J. Heat Transfer* **110,** 1205–1219 (1988).
4. J. R. Ockendon and W. R. Hodgkins, *Moving Boundary Problems in Heat Flow and Diffusion*. Clarendon Press, Oxford (1975).
5. M. C. Flemings and G. E. Nereo, Macrosegregation: part I, *Metall. Soc. AIME* **239,** 1449–1461 (1967).
6. R. Mehrabian, M. Keane and M. C. Flemings, Interdendritic fluid flow and macrosegregation: influence of gravity, *Metall. Trans.* **1,** 1209–1220 (1970).
7. T. Fujii, D. R. Poirier and M. C. Flemings, Macrosegregation in multicomponent low alloy steel, *Metall. Trans.* **10B,** 331–339 (1979).
8. S. D. Ridder, S. Kou and R. Mehrabian, Effect of fluid flow on macrosegregation in axi-symmetric ingots, *Metall. Trans.* **12B,** 435–447 (1981).
9. W. D. Bennon and F. P. Incropera, A continuum model for momentum, heat and species transport in binary solid–liquid phase change systems—I. Model formulation, *Int. J. Heat Mass Transfer* **30,** 2161–2170 (1987).
10. C. Beckermann and R. Viskanta, Double-diffusive convection during dendritic solidification of a binary mixture, *PCH PhysicoChemical Hydrodynamics* **10,** 195–213 (1988).

11. V. R. Voller and C. Prakash, A fixed grid numerical modelling methodology for convection–diffusion mushy region phase-change problems, *Int. J. Heat Mass Transfer* **30,** 1709–1719 (1987).
12. K. C. Chiang and H. L. Tsai, Shrinkage-induced fluid flow and domain change in two-dimensional alloy solidification, *Int. J. Heat Mass Transfer* **35,** 1763–1769 (1992).
13. K. C. Chiang, Studies on the shrinkage-induced transport phenomena during alloy solidification, Appendix A, Ph.D. Dissertation, University of Missouri–Rolla, Rolla, MO (1990).
14. M. K. Walther, Experimental verification of C.A.S.T., *Proc. on Modeling of Casting and Welding Processes*, pp. 345–360, The Metallurgical Society (1986).

INTERACTION ENTRE L'ECOULEMENT INDUIT PAR LE RETRAIT ET LA CONVECTION NATURELLE PENDANT LA SOLIDIFICATION D'UN ALLIAGE

Résumé—On analyse la solidification d'un alliage dans une cavité rectangulaire bidimensionnelle. On présente des résultats dans les trois cas suivants: (1) convection naturelle due à un gradient de température avec domaine constant; (2) écoulement induit par le retrait avec changement de domaine; (3) interaction entre les cas (1) et (2). Pour l'alliage en étude (acier à 1% de Cr), on trouve qu'au début et à la fin de la solidification, l'écoulement induit par le retrait est plus fort que la convection naturelle, tandis que dans la période intermédiaire c'est la convection naturelle qui domine. Aussi l'écoulement fluide causé par le retrait est, dans la zone de boue, plus significative que la convection naturelle, ce qui implique que l'effet du retrait doit être inclus dans la modélisation si on recherche la prédiction des défauts dans le moulage.

WECHSELWIRKUNG VON FLÜSSIGKEITSBEWEGUNG DURCH SCHRUMPFUNGSVORGÄNGE UND NATÜRLICHER KONVEKTION WÄHREND DER ERSTARRUNG VON LEGIERUNGEN

Zusammenfassung—Es wird der zweidimensionale Erstarrungsvorgang von Legierungen in einem Hohlraum mit Steiger untersucht. Die Ergebnisse werden für folgende drei Fälle vorgestellt: (1) natürliche Konvektion infolge von Temperaturgradienten ohne räumliche Veränderung; (2) Flüssigkeitsbewegung durch Schrumpfungsvorgänge mit räumlicher Veränderung; (3) Wechselwirkung zwischen den Fällen (1) und (2). Für die untersuchte Legierung (1% Cr-Stahl) kann gezeigt werden, daß jeweils zu Beginn und am Ende der Erstarrung die Flüssigkeitsbewegung durch Schrumpfung größer ist als diejenige durch Konvektion, während in einem mittleren Bereich die natürliche Konvektion überwiegt. Auch die Bewegung durch Schrumpfung in der Übergangszone ist wichtiger als die durch natürliche Konvektion. Dies bedeutet, daß die Schrumpfungseffekte bei einer zuverlässigen Vorhersage von Gußfehlern nicht vernachlässigt werden dürfen.

ВЗАИМОДЕЙСТВИЕ МЕЖДУ ТЕЧЕНИЕМ ЖИДКОСТИ ЗА СЧЕТ УСАДКИ И ЕСТЕСТВЕННОЙ КОНВЕКЦИИ В ПРОЦЕССЕ ЗАТВЕРДЕВАНИЯ СПЛАВА

Аннотация—Анализируется затвердевание сплавов в двумерной полости прямоугольного сечения. Приводятся результаты для следующих трех случаев: (1) естественная конвекция за счет температурного градиента при постоянстве занятой ею области; (2) обусловленное усадкой течение жидкости при изменяющейся области; (3) сочетание случаев (1) и (2). Для исследуемого сплава (1% хром–сталь) найдено, что на начальной и конечной стадиях затвердевания течение жидкости за счет усадки является более интенсивным, чем естественная конвекция, в то время как на промежуточной стадии доминирует естественная конвекция. Кроме того, вызванное усадкой течение жидкости в переходной зоне более существенно, чем течение за счет естественной конвекции, что указывает на необходимость учета эффекта усадки при моделировании с целью определения дефектов отливки, связанных с течением.